PAPER • OPEN ACCESS

Numerical study of the physical processes of gas leakage in the compression ring in diesel engines

To cite this article: J A Pabón León *et al* 2021 *J. Phys.: Conf. Ser.* **2118** 012016

Numerical study of the physical processes of gas leakage in the compression ring in diesel engines

J A Pabón León[1], J P Rojas Suárez[1], and M S Orjuela Abril[1]
[1] Universidad Francisco de Paula Santander, San José de Cúcuta, Colombia

E-mail: sofiaorjuela@ufps.edu.co

Abstract. In this research, the construction of a numerical model is proposed for the analysis of the friction processes and the thickness of the lubrication film present in the compression ring of internal combustion engines. The model is built using MATLAB software, and three load conditions are used as reference (2 Nm, 4 Nm, and 6 Nm) with a rotation speed of 3600 rpm, which correspond to a stationary single-cylinder diesel engine. Comparison between model estimates and experimental results show that the development model could predict the actual engine conditions. The deviation between the numerical model and the experimental data was 17%. It was shown that the increase in engine load causes a 16% increase in the friction force of the compression ring, which implies a 50% increase in power loss due to friction processes. In general, the model developed allows the analysis of the friction processes in the compression ring and its effect on the lubrication film, considering the leakage of the combustion gases. In this way, the construction of a more complex mathematical model is achieved, which allows improving the precision in the analyzes related to the interaction between the compression ring and the cylinder liner.

1. Introduction

The function of the compression ring is to establish a tight seal between the piston skirt and the cylinder liner; in this way, the leakage of combustion gases is avoided since this type of leakage leads to pressure losses inside the combustion chamber and a reduction in the energy efficiency of the engine. However, high interaction between the compression ring and the cylinder liner causes an increase in friction forces, and therefore a loss in engine power [1,2]. Due to the above, it is necessary to establish an adequate interaction between the cylinder liner and the compression ring. Studies available in the literature show that approximately 11.5% of fuel energy is used to overcome engine friction [3]. It is estimated that the greatest mechanical losses are located in the piston assembly, which represent between 38% – 68% of the total mechanical losses [4]. The piston rings are responsible for 45% of the losses in the piston assembly. Therefore, it can cause a significant deterioration in the performance of the engine [5].

Due to the influence that the interaction between the compression ring and the cylinder liner has on the performance of the engine, it is necessary to use models that allow predicting the energy losses experienced by the engine [6]. In the literature, different formulations with different degrees of complexity are shown to study the behavior of the compression ring; Baelden and Tian [7] used finite element analysis to evaluate the influence of ring deformation on lubricant transport. Baker, *et al.* [8] developed a three-dimensional elasto-dynamic ring model; From the results obtained, it was shown that the dynamics of the piston rings affect the wear of the piston liner, the degradation and consumption of oil, and the formation of hydrocarbon products. Xu, *et al.* [9] indicated that friction processes have direct implications on the surface wear of the cylinder liner. Peng, *et al.* [10] reported that wear and friction between the compression ring and the cylinder liner could cause engine instability. Baker, *et al.* [11] studied the effect of compression of the piston ring on the pressure loss of the combustion chamber. Tian [12] constructed a finite element model to evaluate oil transport and piston ring lubrication. The results indicate that the dynamics of the rings significantly influence the tribological characteristics present in the contact of the cylinder liner and the piston skirt. Additionally, it was concluded that the study of the dynamics of the compression ring is a requirement to accurately understand the power losses of the engine.

Combustion gas leakage is a phenomenon present between the compression ring and the cylinder liner, which affects the dynamic behavior of the ring. This phenomenon causes energy losses, an increase in the temperature of the engine body, and an increase in the oil temperature. Additionally, it causes lubrication disturbances, increased oil consumption, accelerated wear of oil and components, and increased emissions, especially particulate matter and hydrocarbons [5]. Due to the aforementioned, the analysis of the dynamics of combustion gas leaks is essential for a more precise compression of the energy losses present during the combustion process of internal combustion engines.

According to the above, the present investigation proposes the development of a mathematical model to describe the dynamic and tribological characteristics present between the compression ring and the piston liner, considering combustion gas leaks, which are generally neglected in this type of analysis. The foregoing, with the aim of providing physics with a model that allows better precision and understanding of the energy losses caused by the compression ring of the piston.

2. Methodology

This section describes the numerical models used in the study, which involve hydrodynamic lubrication and combustion gas leak models; additionally, the numerical procedure used in the investigation is specified.

2.1. Hydrodynamic lubrication model

The hydrodynamic behavior between the compression ring and the cylinder liner was modeled by using the Reynolds equation, as shown in Equation (1) [13].

$$\frac{\partial}{\partial x}\left(\frac{h^3}{12\mu}\cdot\frac{\partial P}{\partial x}\right)+\frac{\partial}{\partial y}\left(\frac{h^3}{12\mu}\cdot\frac{\partial P}{\partial y}\right)=v_p\cdot\frac{\partial h}{\partial x}+\frac{\partial h}{\partial t}, \tag{1}$$

where P is the pressure distribution, h is the film thickness, μ is the kinematic viscosity and v_p is the sliding velocity; the dynamic viscosity (η) and the density (ρ) of the lubricant are determined from the correlations proposed by Houpert [14] and Dowson–Higginson [15], which are indicated in Equation (2) and Equation (3).

$$\eta=\eta_o\cdot e^{\left[\ln\left(\frac{\eta_o}{\eta_\infty}\right)\times\left(\left\{\frac{T-138}{T_o-138}\right\}^{-s_o}\left\{1+\frac{P-P_o}{c_p}\right\}^{Z}-1\right)\right]}, \tag{2}$$

$$\rho=\rho_o\cdot(1-\gamma[T-T_o])\cdot\left(1+\frac{6\times10^{-10}\cdot(P-P_o)}{1+1.7\times10^{-9}\cdot(P-P_o)}\right), \tag{3}$$

where $c_p=1.98\times10^8$ Pa and $\eta_\infty=6.31\times10^{-5}$ Pa $\cdot$ s are constants of the model, s_o is the thermo-viscosity index, Z is the piezo-viscosity index, and γ is the coefficient of thermal expansion of the lubricant. The subscript o indicates atmospheric conditions. The sliding velocity (v_p) of the compression ring is considered equal to the velocity of the piston. Therefore, v_p can be determined by Equation (4) [16].

$$v_p=r\cdot\omega\cdot\sin\theta+\frac{r\cdot\omega\cdot\sin\theta\cdot\cos\theta}{\sqrt{\frac{l}{r}-\sin^2\theta}}, \tag{4}$$

where r is the crank radius, ω is the crankshaft angular velocity, l is the connecting rod length, and θ is the crank angle. The power loss (P_l) in the compression ring is determined by Equation (5) [17].

$$P_l = (f_v + f_b) \cdot |v_p|, \tag{5}$$

where f_v is the viscous friction and f_b is the ring boundary friction, respectively.

2.2. Combustion gas leak model

As the pressure inside the combustion chamber increases, the combustion gases tend to be directed into the grooves between the compression ring and the piston. The mass flow rate ($\dot{m}_g$) is determined considering an isentropic behavior, as shown in Equation (6) [18].

$$\dot{m}_g = f_m \frac{A_g \cdot C_f \cdot P_u}{\sqrt{R \cdot T_u}}, \tag{6}$$

where C_f is the coefficient of discharge, A_g is the downstream ring end gap area, f_m is the compressibility factor, T_u is the orifice upstream temperature, R is the ideal gas constant and P_u is the gas pressure upstream. The coefficient of discharge (C_f) and the compressibility factor (f_m) are calculated by Equation (7) and Equation (8) [18].

$$C_f = 0.85 - 0.25 \left(\frac{P_d}{P_u}\right)^2, \tag{7}$$

$$f_m = \left\{ \begin{array}{l} \sqrt{\gamma} \cdot \left(\frac{2}{\gamma+1}\right)^{\frac{\gamma+1}{2(\gamma-1)}}, \ \frac{P_d}{P_u} > \left(\frac{2}{\gamma+1}\right)^{\frac{\gamma}{(\gamma-1)}} \\ 0.85 - 0.25 \left(\frac{P_d}{P_u}\right)^2, \ \frac{P_d}{P_u} > \left(\frac{2}{\gamma+1}\right)^{\frac{\gamma}{(\gamma-1)}} \end{array} \right\}, \tag{8}$$

where P_d is the gas pressure downstream, and γ is the ratio of the specific heats; the power loss associated with the leak of combustion gases (P_k) is determined by Equation (9) [19].

$$P_k = \frac{\dot{m}_g \cdot R \cdot T_u \cdot \gamma}{\gamma - 1} \cdot \left(1 - \left[\frac{P_d}{P_u}\right]^{\frac{\gamma-1}{\gamma}}\right). \tag{9}$$

2.3. Numerical procedure

The equations described in section 2.1 and section 2.2, are solved using the ode45 solver of the MATLAB software; Figure 1 describes the flow diagram of the numerical model.

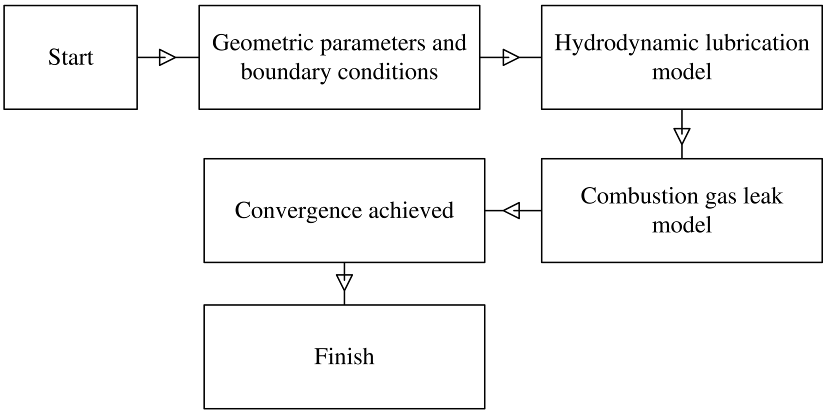

Figure 1. Numerical model flow diagram.

The reference conditions of the numerical model are based on the technical and operational characteristics of a stationary single-cylinder diesel engine. The properties of the engine are described in Table 1. A constant rotational speed of 3600 rpm and three load conditions (2 Nm, 4 Nm, and 6 Nm) were selected for the numerical analysis of the engine.

Table 1. Technical specifications of the engine.

Characteristics	Value
Model	SK – MDF 300
Manufacturer	SOKAN
Stroke	63 mm
Bore	78 mm
Intake system	Naturally aspirated
Displaced	300 cc
Injection system	Direct injection

3. Results

This section describes the results and discussions obtained for the present investigation; the analysis carried out includes the evaluation of the friction force and the analysis of the loss power associated with this force. Additionally, a study of the change in the thickness of the lubrication film is carried out, as well as the pressure conditions present in the compression ring.

3.1. Experimental validation

To guarantee the reliability of the model, a comparison was made with the friction force during the combustion cycle measured experimentally. This measurement was carried out with a rotation speed of 3600 rpm and a load of 6 Nm. The results of the comparison between the model and experimental data are shown in Figure 2.

From Figure 2, it was observed that the model could represent the real behavior experienced by the compression ring of the engine. The adequate similarity was evidenced in both magnitude and trend between the model and the experimental data. Analysis of the mean relative error shows a deviation of 17%. Due to the difficulty for the actual measurement of the friction force on the piston, the error reached is considered adequate [20].

The analysis of the pressure inside the combustion chamber throughout the combustion cycle is indicated in Figure 3 for the load conditions of 2 Nm, 4 Nm, and 6 Nm. The results indicate that pressure tends to increase with increasing engine load levels. In general, it was observed that a 2 Nm increase in engine load causes an 11% increase in peak combustion pressure. This may imply greater ease of combustion gas leakage and greater power losses due to friction processes between the compression ring and the cylinder liner.

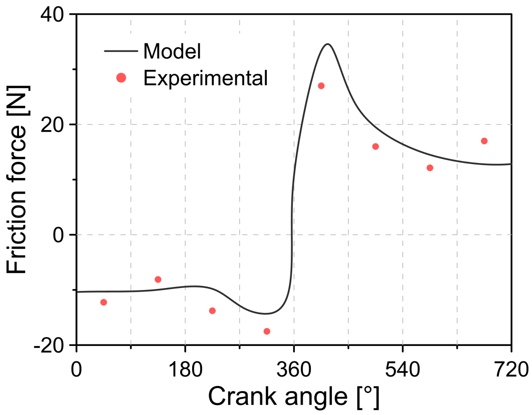

Figure 2. Comparison between the friction force obtained experimental vs. model.

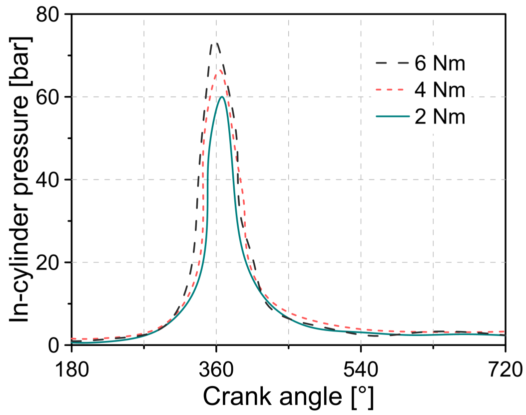

Figure 3. Average pressure of the pneumatic network.

Figure 4 shows the influence of the engine load on the friction force present in the compression ring; it was observed that the maximum magnitude of the friction force occurs during the expansion process (360° – 540°) for all load conditions. This can be attributed to the reduction in the lubrication film and the high acceleration experienced by the piston during this stage. In general, the increase in engine load causes an increase in the friction force. For the load conditions of 2 Nm, 4 Nm, and 6 Nm, a maximum force of 25.6%, 29.4%, and 34.8% was recorded, respectively.

The friction force causes a loss of power, which can be seen in Figure 5. Increasing the engine load tends to increase the loss of engine power. This is directly associated with the greater magnitude of the friction force, as shown in Figure 4. In general, the greatest losses occur during the middle of each stage of combustion. This is due to the mixed lubrication regime condition present during these parts of the cycle.

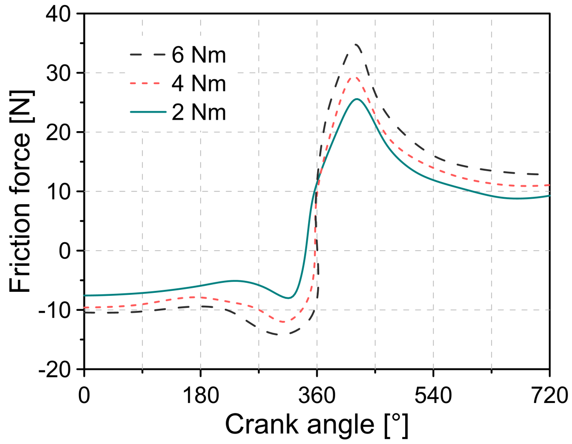

Figure 4. Friction force for different load conditions.

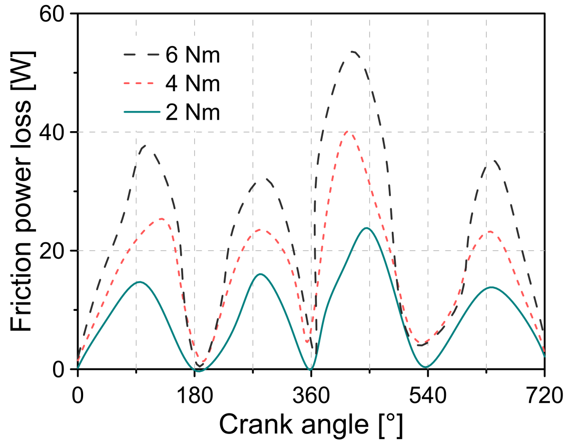

Figure 5. Friction power loss for different load conditions.

Figure 6 indicates the minimum lubrication film thickness during the combustion cycle for different load conditions. In general, the smallest thickness of the lubrication film was located at the angles of 180°, 360°, 540°, and 720°, which coincide with the change in the direction of movement of the piston. This facilitates the formation of a mixed lubrication regime, and therefore, the reduction in the minimum thickness of the lubrication film. A minimum lubrication film thickness of 1.50 μm, 2.19 μm, and 3.23 μm was reported for a load of 2 Nm, 4 Nm, and 6 Nm, respectively.

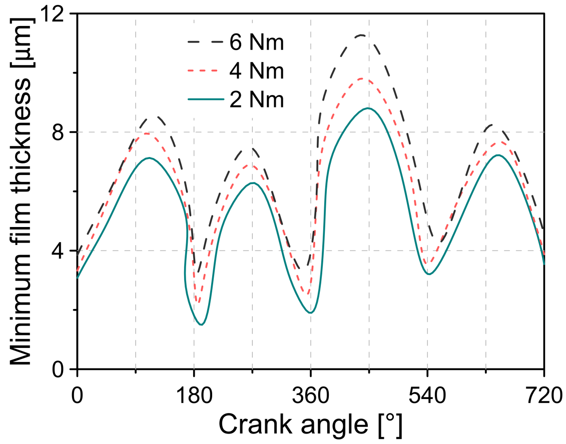

Figure 6. Minimum film thickness for different load conditions.

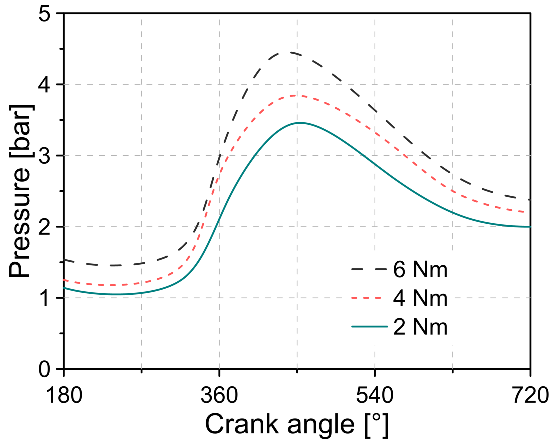

Figure 7. Pressure in the combustion chamber in the bottom groove of the ring.

Figure 7 indicates the localized pressure in the bottom groove between the compression ring and the piston during the combustion cycle. From the results obtained, it is shown that the pressure curves present a similar behavior for the different load conditions. The maximum pressure peak was located approximately at an angle of 440°, which corresponds to the descent of the piston during the expansion stage; for a load of 2 Nm, 4 Nm, and 6 Nm, maximum pressure of 3.45 bar, 3.83 bar, and 4.44 bar was obtained, respectively. This pressure increase implies a greater amount of flow gas leakage.

4. Conclusions

In this research, the development of a numerical model for the analysis of the friction processes experienced by the compression ring is proposed, considering the hydrodynamic lubrication characteristics and the combustion gas leaks present in the combustion chamber jointly. The development of the model was carried out using MATLAB software, taking as reference three load conditions (2Nm, 4 Nm, and 6 Nm) with a rotation speed of 3600 rpm.

Comparison between model estimates and experimental results show that the development model could predict the actual engine conditions. In general, the deviation between the numerical model and the experimental data was 17%, which is acceptable for the type of study carried out. The model allowed the analysis of friction forces and the associated energy loss during the combustion cycle. The increase in engine load was shown to cause a 16% increase in the friction force of the compression ring. The above implied an increase of approximately 50% in the power loss due to friction processes. The model allowed to analyze the minimum thickness of the lubrication film, showing that the change in the direction of the piston movement causes the greatest risk of wear in the engine. For the load conditions of 2 Nm, 4 Nm, and 6 Nm, a minimum lubrication thickness of 1.50 μm, 2.19 μm, and 3.23 μm, was reported, respectively. Additionally, it was observed that the increase in engine load causes a 15% increase in the pressure of the bottom ring groove.

In general, the model developed allows the analysis of the friction processes in the compression ring and its effect on the lubrication film, considering the leakage of the combustion gases, which is usually ignored in this type of analysis. In this way, the construction of a more complex mathematical model is achieved, which allows improving the precision in the analyzes related to the interaction between the compression ring and the cylinder liner.

References

[1] Consuegra F, Bula A, Guillín W, Sánchez J, Duarte Forero J 2019 Instantaneous in-cylinder volume considering deformation and clearance due to lubricating film in reciprocating internal combustion engines *Energies* **12(8)** 1437
[2] Hernández B, Maestre D, Pardo C, Fonseca M D S, Pabón J 2021 Influence of compression rings on the dynamic characteristics and sealing capacity of the combustion chamber in diesel engines *Lubricants* **9(3)** 25
[3] Holmberg K, Andersson P, Erdemir A 2012 Global energy consumption due to friction in passenger cars *Tribology International* **47** 221
[4] Tormos B, Martin J, Pla B, Jimenez-Reyes A J 2020 A methodology to estimate mechanical losses and its distribution during a real driving cycle *Tribology International* **145** 106208
[5] Koszalka G, Hunicz J 2021 Comparative study of energy losses related to the ring pack operation in homogeneous charge compression ignition and spark ignition combustion *Energy* **235** 121388
[6] Forero J D, Ochoa G V, Alvarado W P 2020 Study of the piston secondary movement on the tribological performance of a single cylinder low-displacement diesel engine *Lubricants* **8(11)** 97
[7] Baelden C, Tian T 2014 A dual grid curved beam finite element model of piston rings for improved contact capabilities *SAE International Journal of Engines* **7(1)** 156
[8] Baker C, Rahmani R, Theodossiades S, Rahnejat H, Fitzsimons B 2015 On the effect of transient in-plane dynamics of the compression ring upon its tribological performance *Journal of Engineering for Gas Turbines and Power* **137(3)** 032512
[9] Xu Y, Zheng Q, Geng J, Dong Y, Tian M, Yao L, Dearn K D 2019 Synergistic effects of electroless piston ring coatings and nano-additives in oil on the friction and wear of a piston ring/cylinder liner pair *Wear* **422** 201

[10] Peng Y, Xu Y, Geng J, Dearn K D, Hu X 2017 Tribological assessment of coated piston ring-cylinder liner contacts under bio-oil lubricated conditions *Tribology International* **107** 283
[11] Baker C, Rahmani R, Karagiannis I, Theodossiades S, Rahnejat H, Frendt A 2014 Effect of compression ring elastodynamics behaviour upon blowby and power loss *SAE Technical Paper* **2014-01-1669** 1
[12] Tian T 2002 Dynamic behaviours of piston rings and their practical impact. Part 2: Oil transport, friction and wear of ring/liner interface and the effects of piston and ring dynamics *Proceedings of the Institution of Mechanical Engineers, Part J: Journal of Engineering Tribology* **216(4)** 229
[13] Patir N, Cheng H S 1978 An average flow model for determining effects of three-dimensional roughness on partial hydrodynamic lubrication *Journal of Lubrication Technology* **100(1)** 12
[14] Houpert L 1985 New results of traction force calculations in elastohydrodynamic contacts *Journal of Tribology* **107(2)** 241
[15] Dowson D, Higginson G R 1959 A numerical solution to the elasto-hydrodynamic problem *Journal of Mechanical Engineering Science* **1(1)** 6
[16] Rahnejat H 2005 *Multi-Body Dynamics. Vehicles, Machines, and Mechanisms* (Bury St Edmunds: John Wiley & Sons Ltd)
[17] Zavos A, Nikolakopoulos P G 2021 Investigation of the top compression ring power loss and energy consumption for different engine conditions *Tribology-Materials, Surfaces & Interfaces* 1
[18] Kurbet S N, Kumar R K 2007 Finite element modelling of piston-ring dynamics and blow-by estimation in a four-cylinder diesel engine *Proceedings of the Institution of Mechanical Engineers, Part D: Journal of Automobile Engineering* **221(11)** 1405
[19] Woods W A 1991 On the role of the harmonic mean isentropic exponent in the analysis of the closed-cycle gas turbine *Proceedings of the Institution of Mechanical Engineers, Part A: Journal of Power and Energy* **205(4)** 287
[20] Gore M, Theaker M, Howell-Smith S, Rahnejat H, King P D 2014 Direct measurement of piston friction of internal-combustion engines using the floating-liner principle *Proceedings of the Institution of Mechanical Engineers, Part D: Journal of Automobile Engineering* **228(3)** 344